SLAC-PUB-756
May 1970
(TH) and (EXP)

FOURTH ORDER ELECTRODYNAMIC CORRECTIONS TO THE LAMB SHIFT†

Thomas Appelquist

and

Stanley J. Brodsky

Stanford Linear Accelerator Center, Stanford University, Stanford, California 94305

ABSTRACT

The fourth-order radiative correction to the slope at $q^2 = 0$ of the Dirac form factor of the free electron vertex is calculated using computer techniques. The result,

$$m^2 \partial F_1^{(4)}(0)/\partial q^2 = (\alpha/\pi)^2 [0.48 \pm 0.07],$$

disagrees with previous calculations, and implies a new theoretical value for the order $\alpha^2(Z\alpha)^4 mc^2$ contribution to the Lamb shift. The new values for the $2S_{\frac{1}{2}} - 2P_{\frac{1}{2}}$ separation in H and D are increased by (0.35 ± 0.07) MHz and are in good agreement with the results of recent experiments.

(Submitted to The Physical Review)

---

† Work supported by the U. S. Atomic Energy Commission.

I. INTRODUCTION

The calculations and measurements of the Lamb shift have had a profound influence on the development of quantum electrodynamics. The first measurements of the $2S_{\frac{1}{2}}$ level displacement from the $2P_{\frac{1}{2}}$ level in hydrogen by Lamb and Retherford[1] stimulated the concept of mass renormalization and led Bethe[2] to carry out the first finite calculation of the self-interaction of the electron with the quantized electromagnetic field. The relativistic theory that emerged has met all of its experimental challenges with great quantitative success;[3] the agreement is better than 10 ppm for the hyperfine splitting of hydrogen and muonium and better than 0.1 ppm in the total magnetic moments of the electron and muon.

Ironically, the only tests of QED which show a serious disagreement ($\gtrsim 200 \pm 70$ ppm) between theory and experiment are the $2S_{\frac{1}{2}} - 2P_{\frac{1}{2}}$ separations in hydrogen and deuterium. The disagreement has become more acute with recent measurements by Robiscoe and Cosens[4] and others[5] of the Lamb interval in H, D, He^{+}, Li^{++}, and three measurements[6] of the $2P_{\frac{3}{2}} - 2S_{\frac{1}{2}}$ interval in H. The latest experimental results are shown in Table I. The theoretical predictions have become more precise over the years with the development of new calculational techniques by Layzer[7], Karplus, Klein, and Schwinger[8], and Erickson and Yennie[9] for the evaluation of the order α (second order in perturbation theory) self-energy expression for the Coulomb-bound electron. In addition, the nuclear recoil corrections (m/M contributions beyond reduced mass effects) originally evaluated by Salpeter[10] from the Bethe-Salpeter equation have now been checked by Grotch and Yennie[11] using an effective potential technique. The various contributions to the theoretical prediction of the $2S_{\frac{1}{2}} - 2P_{\frac{1}{2}}$ separation in H are shown in column one of Table II. The total result , 1057.56 ± 0.09 MHz ("limit of error") is in clear disagreement with the experimental numbers in Table I. The corresponding result for D, 1058.82 ± 0.15 MHz is in similar disagreement. The only experimentally relevant contribution in the table, not checked by independent methods, is the fourth order electron self-energy correction proportional to the slope of the Dirac form factor at $q^2 = 0$, labeled $F_1'(0)$. This contribution was first estimated by Weneser, Bersohn and Kroll[12] and calculated completely analytically by Soto[12].

In this paper we present the details of a new calculation[13] of this fourth order $[\alpha^2 (Z\alpha)^4 m]$ radiative contribution to the Lamb shift. Our result differs from the previous calculation of Soto[12] and, when added to the other contributions of Table II, leads to new theoretical values for the Lamb shift in H and D of 1057.91 ± 0.16 and 1059.17 ± 0.22 MHz respectively, an increase of 0.35 ± 0.07 MHz over the previous compilation of Taylor et al.[4] A tabulation of the various contributions to the theoretical result for H, including the revised fourth order contribution of $F_1'(0)$, is given in Table II. The comparison of the revised theory with experiment is given in the last column of Tables Ia and Ib. The majority of the experimental results are within one standard deviation of theory, leaving only one high precision measurement,[5] which uses the non-atomic beam "bottle" method, in serious disagreement. The one standard deviation error limits used in the comparison of theory and experiment were computed by combining the standard deviation experimental error assigned by Taylor et al.[4] with one-third of the limit of error (L.E.) of the theoretical result.

II. DESCRIPTION OF THE CALCULATION

In principle, one must compute radiative corrections to atomic energy levels using bound state perturbation theory. Instead, for the terms of interest here, the $\alpha^2 (Z\alpha)^4 m$ contribution, we can use the so-called scattering approximation[12,14] which is calculationally simpler. In this approach, one calculates the radiative corrections to the scattering of a free electron and then infers from this a modified interaction potential from which the level shifts can be calculated.

The matrix element of the electromagnetic current between two free electron states is given by[15]

$$- ie\bar{u}\,(p + \tfrac{q}{2})\left[\gamma_\mu F_1(q^2) + \frac{1}{4m}[\not{q}\,, \gamma_\mu]\, F_2(q^2)\right] u(p - \tfrac{q}{2}) \tag{2.1}$$

The modification of the Coulomb interaction due to $F_1(q^2)$ implies an energy shift

$$\Delta E(n, j, \ell) \;=\; \delta_{\ell o} \frac{4(Z\alpha)^4 mc^2}{n^3} \; m^2 \left.\frac{\partial F_1(q^2)}{\partial q^2}\right|_{q^2 = 0} \tag{2.2}$$

plus contributions of higher order in the binding parameter $Z\alpha$. In second order,

$$m^2 \left.\frac{\partial F_1^{(2)}(q^2)}{\partial q^2}\right|_{q^2 = 0} \;=\; \frac{\alpha}{3\pi}\left[\log\frac{m}{\lambda} - \frac{3}{8}\right] \quad (\lambda << m) \tag{2.3}$$

is infrared divergent for a free electron. This divergence reflects the fact that the scattering approximation is invalid for the order α contribution. In the correct bound-state treatment of the low frequency region, the photon mass

λ is replaced by an appropriate energy difference, the Bethe energy $|E_n - E_m|_{av}$, and Eq. (2.2) with (2.3) gives the dominant contribution to the Lamb shift. Photons of wavelengths much larger than atomic dimensions do not contribute to the energy shift since they contribute equally to the self-energy of free and bound electrons.

The order α^2 contribution to the slope of the Dirac form factor was first shown to be convergent in the infrared by Weneser, Bersohn and Kroll[12,16]. This result was verified by Mills and Kroll[14] starting from the fourth order self-energy expression for the energy shift of the bound electron. These authors have also given an explicit proof that the scattering approximation is correct in fourth-order. Soto[12] was able to perform the required integrals analytically (including those only bounded by WBK) and found some small errors in WBK's work. His result was

$$m^2 \left.\frac{\partial F_1^{(4)}}{\partial q^2}\right|_{q^2=0} = \frac{\alpha^2}{\pi^2} [0.1076 \ldots] \tag{2.4}$$

which yields the contribution 0.102 MHz to the $2S_{\frac{1}{2}} - 2P_{\frac{1}{2}}$ separation in H and D. Other fourth-order contributions to the Lamb shift from $F_2(0)$ and vacuum polarization corrections are included in the tabulation of Table II. Contributions of order q^4 from $F_1(q^2)$ and vertex-vacuum polarization cross terms yield corrections one order of $Z\alpha$ smaller.

The Feynman diagrams which are required to calculate the fourth order contribution to the slope $F_1'(0)$ are shown in Figure 1. The calculational and renormalization techniques are similar to those used in magnetic moment $F_2(0)$ calculations of Karplus and Kroll[17] and Petermann[18], although the slope calculation involves more complicated numerator structures and contributions from differentiation of denominators with respect to q^2. Furthermore, in the standard gauge, individual graphs have $\log^2\lambda$ and $\log\lambda$ behavior in the infrared region of photon integration, although the complete fourth order result is infrared convergent.[16] In the calculation presented in this paper, all traces, projections, and reduction to Feynman parametric integrals are done automatically by REDUCE, an algebraic computation program written by A. C. Hearn[19]. The definitions of the required subsidiary variables in terms of the Feynman parameters are obtained by alternate methods, the standard technique given in Ref. (15) and the method developed by Nakanishi and others[20]. The integrals over the Feynman parameters (up to five dimensions) are performed numerically (often to 0.1% precision) using a program originally written by G. Sheppey and modified by A. J. Dufner. In this method of multi-dimensional integration, more fully described in Ref. (21), one calculates the usual Riemann sum, taking the central value of the integrand from an average over two random points within each hypercube. The difference of the function values is used to compute a variance and error for the integration; on successive iterations the computer readjusts the grid to minimize the variance. Many of the techniques used in this paper are similar to those used by Aldins et al.[21], for the calculation of the photon-photon scattering contribution to the sixth order electron and muon magnetic moments.

Our numerical result for the fourth order slope is

$$m^2 \left.\frac{\partial F_1^{(4)}}{\partial q^2}\right|_{q^2=0} = \frac{\alpha^2}{\pi^2}\,[0.48 \pm 0.07] \tag{2.5}$$

The contributions of the individual graphs are tabulated in Table III. The discrepancy with the results of Ref. (12) originates in an overall sign disagreement and in the calculation of the constant terms in the crossed and corner graphs (see Figures Ia and Ib). In the case of the corner graph, this discrepancy is quite large. The revised theoretical values for the Lamb shifts in H, D, He^+ and Li^{++} are shown in Tables Ia and Ib.

III. VACUUM POLARIZATION AND FERMION SELF-ENERGY INSERTIONS

The contribution of the graph with the second order vacuum polarization insertion (Figure Ic) is easiest to calculate and we start our discussion here. The effect of second order vacuum polarization is summarized by a modification to the photon propagator[22]

$$\frac{1}{k^2-\lambda^2+i\epsilon} \rightarrow \frac{1}{k^2-\lambda^2+i\epsilon} + \frac{\alpha}{\pi}\int_0^1 dz\, \frac{z^2(1-\frac{1}{3}z^2)}{1-z^2}\, \frac{1}{k^2-\frac{4m^2}{1-z^2}+i\epsilon} \tag{3.1}$$

Note that the second order contribution to the slope of the Dirac form factor

$$m^2 \left.\frac{\partial F_1^{(2)}}{\partial q^2}\right|_{q^2=0} = \frac{\alpha}{2\pi}\int_0^1 v\,dv\, \frac{\frac{2}{3}v^2 + 1-v) + \frac{1}{2}v^4 + \frac{\lambda^2}{m^2}(1-v)(1-v+\frac{v^2}{3})}{\left[v^2+\frac{\lambda^2}{m^2}(1-v)\right]^2} \tag{3.2}$$

is positive for all λ^2. Insertion of (3.1) is effectively a sum over various λ^2 with a positive weight function. The vacuum polarization contribution to a_4 is thus of the same sign as the second order slope and hence gives a positive Lamb shift contribution. (Thus, as is usual, the vacuum polarization modification strengthens the contribution of one-photon exchange.) Upon numerical integration, we obtain

$$a_4(\text{V.P.}) = 0.0316 \pm 0.0002 \tag{3.3}$$

in contrast to a negative Lamb shift contribution of the same magnitude in Refs. (12) and (13).

The fermion self-energy correction (Figure Id) is accomplished by substituting

$$\frac{1}{\not{p} - m + i\epsilon} \rightarrow \Sigma_f(p) \tag{3.4}$$

in each leg of the second order vertex. Here Σ_f is the twice-subtracted part of the self-energy insertion:

$$\Sigma(p) = A + (\not{p} - m)B + (\not{p} - m)^2 \Sigma_f(p) \tag{3.5}$$

$$\Sigma_f(p) = \frac{\alpha}{2\pi} \int_0^1 dx \int_0^1 dz \; \frac{\omega(x,z)\,[\not{p} + \mathcal{M}(x,z)]}{p^2 - r(x,z)\,m^2 + i\epsilon} \tag{3.6}$$

where

$$\begin{aligned} \omega &= s(1-x)/z \\ r &= [x(1-x)z + \frac{\lambda^2}{m^2}(1-x) + x^2]/[x(1-x)z] \\ \mathcal{M} &= m[s(1-x) - (1+x)]/[s(1-x)] \\ \text{and} \qquad s &= 1 - 2\,z(1+x)\,x/[x^2 + (1-x)\lambda^2/m^2] \;. \end{aligned} \tag{3.7}$$

It should be emphasized that great care must be used in extracting Σ_f to keep all terms in λ^2.[23]

The method of calculation is similar to that for the graph with vacuum polarization insertion. The second order contribution to $F_1'(0)$ with one fermion propagator replaced by

$$\frac{\not{p} + \mathcal{M}(x,z)}{p^2 - r(x,z)\,m^2 + i\epsilon}$$

is

$$m^2 \left.\frac{\partial F_1^{(2)}(q^2, \mathcal{M}, r)}{\partial q^2}\right|_{q^2=0} = \frac{\alpha}{2\pi} \int_0^1 dz_1\, dz_2\, dz_3\, \delta(1 - z_1 - z_2 - z_3)$$

$$\left\{ \frac{z_2 z_3 + (1-z_2)(1-z_3)}{(1-z_1)^2 + z_1 \frac{\lambda^2}{m^2} + (r-1) z_2} + \frac{(\frac{\mathcal{M}}{m} - 4z_1 + z_1^2) z_2 z_3}{[(1-z_1)^2 + z_1 \frac{\lambda^2}{m^2} + (r-1) z_2]^2} \right\} . \tag{3.8}$$

Then $\partial F^{(4d)}/\partial q^2)\Big|_{q^2=0}$ is given by

$$m^2 \left.\frac{\partial F^{(4d)}}{\partial q^2}\right|_{q^2=0} = \frac{\alpha}{\pi} \int_0^1 dx \int_0^1 dz\;\omega(x,z) \left.\frac{\partial F_1^{(2)}(q^2, \mathcal{M}, r)}{\partial q^2}\right|_{q^2=0} \tag{3.9}$$

where a factor of 2 is included for the mirror graph. This integral is easily carried out numerically for various λ^2 and can be compared as $\lambda^2 \to 0$ with the analytic result of WBK[12] and Soto[13]

$$m^2 \left.\frac{\partial F^{(4d)}}{\partial q^2}\right|_{q^2=0} \underset{\lambda \ll m}{=} \frac{1}{12} \log^2 \frac{m^2}{\lambda^2} - \frac{1}{72} \log \frac{m^2}{\lambda^2} - 1.688 \ldots \quad . \tag{3.10}$$

The result for our calculations is shown in Figure II. As seen in Figure II, apart from an overall sign, excellent agreement is obtained.

The common feature that the actual dependence of the integrals pulls appreciably away from the asymptotic formula even at λ^2 as small as $10^{-3} m^2$ reflects the fact that Eq. (3.9) is a negative function of λ^2 for all positive λ^2 and does not cross the axis as the extrapolated asymptotic formulas do.

IV. THE CORNER GRAPH

In calculating the contributions from the graphs with vacuum polarization and fermion self-energy insertions, we followed the procedure of first calculating the renormalized amplitudes for the subgraphs, inserting their spectral integral representations into the second order vertex graphs and then doing the over-all renormalization subtractions.

It is also possible to use a similar procedure[12] for the corner graph of Figure Ib (and the ladder graph to be treated in the next section). However, the integral representation for the renormalized vertex subgraph is much more complicated than that for self-energy graphs, requiring in general a dispersion representation in the three off-shell variables. We have used instead a different approach which is simpler, at least when the computer is used for the algebraic reduction and numerical evaluation of the integrals. It will be helpful to first outline the method and then present it in detail. We first combine all the denominators of the unrenormalized amplitudes and project out the Dirac form factor F_1. The internal momentum integrations are then done and the result is expressed as a five dimensional integration over parameters. The ultraviolet divergences corresponding to the vertex subgraph and to the graph as a whole will, of course, still be present in the parametric integral. The subtraction necessary to remove the internal logarithmic divergence is implemented by recomputing this expression with the vertex subgraph computed with the external momenta which flow through it constrained to the mass shell, again combining all six denominators first. The integrands are then subtracted and the resulting five dimensional integral will contain only the overall divergence, which is subtracted automatically at $q^2 = 0$ when we compute $F_1'(0)$. Once the difference of integrands is differentiated with respect to q^2 and q^2 is set equal to zero, the result (for $\lambda^2 > 0$) is a convergent five dimensional integral for $F_1'(0)$ which we can evaluate numerically by computer. We shall describe several checks on the calculations of $F_1'(0)$ including the evaluation of corner and crossed graph contributions to $F_2(0)$.

The unrenormalized amplitude for the corner graph is

$$
\begin{aligned}
M^\nu_{\text{corner}} &= 2(-ie)^5\, i^4 (-i)^2 \int \frac{d^4\ell_1}{(2\pi)^4} \frac{d^4\ell_2}{(2\pi)^4} \frac{1}{\prod_{i=1}^{6} (p_i^2 - m_i^2)} \\
&\quad \times \bar{u}(p+\tfrac{q}{2}) \left[\gamma_\beta (\not{p}_4 + m)\, \gamma^\nu (\not{p}_3 + m)\, \gamma_\alpha (\not{p}_2 + m)\, \gamma^\beta (\not{p}_1 + m)\, \gamma^\alpha \right] u(p - \tfrac{q}{2}) \qquad (4.1) \\
&= -ie\, \bar{u}(p + \tfrac{q}{2})\, J^\nu_{\text{corner}}\, u(p - \tfrac{q}{2}) .
\end{aligned}
$$

The factor of two is included for the mirror graph.

We can automatically determine the contribution to the form factors (see Eq. (2.1)) through

$$F_j(q^2) = \tfrac{1}{4}\, T_r \left[(\not{p} + \frac{\not{q}}{2} + m)\, J^\mu\, (\not{p} - \frac{\not{q}}{2} + m)\, \Lambda_\mu^{(j)} \right] \tag{4.2}$$

where[25]

$$\Lambda_\mu^{(1)} = \left[3m\, p_\mu - p^2 \gamma_\mu \right] \frac{1}{4p^4} \tag{4.3}$$

$$\Lambda_\mu^{(2)} = \left[m^2 p^2 \gamma_\mu - m(m^2 + q^2/2)\, p_\mu \right] \frac{1}{q^2 p^4} \tag{4.4}$$

with

$$p^2 = m^2 - q^2/4, \qquad p \cdot q = 0 \tag{4.5}$$

After the traces and index contractions are performed to obtain $F_1(q^2)$ we have to consider integrals of the form

$$I = \int \frac{d^4\ell_1\, d^4\ell_2}{\prod_{i=1}^{6} (p_i^2 - m_i^2 + i\epsilon)} \quad F(p_j) \tag{4.6}$$

where m_i is the mass corresponding to line i and

$$p_j = k_j + \sum_{r=1}^{2} \eta_{jr} \ell_r \qquad (j = 1, \ldots, 6) \tag{4.7}$$

Here η_{jr} is the projection ($\pm$ 1, 0) of p_j along ℓ_r and k_j can be any choice of fixed momenta (independent of ℓ_r, proportional to p, q) such that four-momentum is retained at the five vertices. Feynman parameters are now introduced

$$\frac{1}{\prod_{j=1}^{6} (p_j^2 - m_j^2 + i\epsilon)} = 5! \int \frac{dz_1 \ldots dz_6\, \delta\left(1 - \sum_{i=1}^{6} z_i\right)}{\left[\sum_j z_j (p_j^2 - m_j^2 + i\epsilon)\right]^6} \tag{4.8}$$

If we choose the k_j such that[15]

$$\sum_{j=1}^{6} z_j k_j \eta_{jr} = 0 \qquad (r = 1, 2) \tag{4.9}$$

then the $k_j \cdot \ell_r$ cross terms in the denominator vanish. For convenience we define

$$U = \det U_{rr'}, \qquad U_{rr'} = \sum_{j=1}^{6} z_j \eta_{jr} \eta_{jr'} \tag{4.10}$$

and

$$D = \sum_{j=1}^{6} z_j (m_j^2 - k_j^2) \tag{4.11}$$

The basic integration over loop moment q then gives

$$5! \int \frac{d^4\ell_1 \, d^4\ell_2}{\left[-D + \sum_{rr'} U_{rr'} \, \ell_r \cdot \ell_{r'} + i\epsilon\right]^6} = \frac{i^2 \pi^4}{D^2 U^2} \tag{4.12}$$

The numerator also contains terms quadratic and quartic in the loop momentum four vectors. For the $\ell_a \cdot \ell_b$ terms[21] we replace

$$\ell_a \cdot \ell_b \longrightarrow -2B_{ab} \frac{D}{U} \tag{4.13}$$

where B_{ab} is the signed co-factor of U_{ab} in U. Also

$$\ell_a \cdot \ell_b \, \ell_c \cdot \ell_d \longrightarrow \left[4B_{ab}B_{cd} + B_{ad}B_{bc} + B_{ac}B_{bd}\right] \frac{D^2}{U^2} \left[\log \frac{\Lambda^2}{D} + 1\right]. \tag{4.14}$$

The dependence on the ultraviolet cutoff Λ^2 is eliminated because of the overall subtraction at $q^2 = 0$, and we can in fact replace

$$1 + \log \frac{\Lambda^2}{D(q^2)} \longrightarrow \log \frac{D(q^2 = 0)}{D(q^2)} \tag{4.15}$$

These substitutions can also be readily done by REDUCE[19] yielding the reduction of the matrix element to an integrand for parametric integration (in the form of a punched deck in Fortran form). The program which produces the integrand for the corner graph is shown in Figure 3.

As an alternate method to the above and as a check we have also used the graphical method of reduction to parametric form developed by Nakanishi[20] and others. A particularly valuable check is obtained for the quantity

$$U \sum_{j=1}^{6} z_j k_j^2 = W_p m^2 + W_q q^2 \tag{4.16}$$

in which the parametric functions W_p and W_q can be read off very simply from the Feynman graph structure. The definitions of all the subsidiary quantities k_j, W_p, W_q, U in terms of $z_1 \ldots z_6$ for the corner graph are given in Figure 4 which is the actual Fortran program used as the integrand for the numerical integration of $F_1'(0)$ over five dimensions.

The internal vertex renormalization subtraction must yet be performed. Thus we subtract from M^{ν}_{corner} the corresponding amplitude with the internal loop calculated as if lines 3 and 6 (see Figure 1b) were on their respective mass shell:

$$M^{\nu}_{\text{corner sub}} = 2(-ie)^5 i^4 (-i)^2 \int \frac{d^4\ell_1}{(2\pi)^4} \bar{u} \frac{\gamma_\alpha(\not{p}_4 + m)\gamma^{\nu}(\not{p}_3 + m)\gamma^{\alpha}}{\prod_{j=3,4,6} (p_j^2 - m_j^2)} u$$

$$\times \int \frac{d^4\ell_2}{(2\pi)^4} \frac{\frac{1}{4}\mathrm{Tr}\left[\gamma_\beta(\not{p}_2 + m)\not{R}(\not{p}_1 + m)\gamma^{\beta}(\not{R} + m)\right]}{m^2 \prod_{j=1,2,5} (p_i^2 - m_j^2)} \tag{4.17}$$

where $p_1 + p_5 = p_2 + p_5 = R$
and $R^2 = m^2$. The corresponding integrand and modification to the definition of U, k_j, W_p, W_q are shown in Figure 4 . This integrand is then subtracted from the above before numerical evaluation of the five-dimentional integral. The subtraction is sufficient to remove the ultraviolet divergence associated with the vertex subgraph which appears as logarithmic singularity as $z_1, z_2, z_5 \to 0$. The over all divergence, characterized by the Λ^2 in Eq. (4.14) is removed automatically when we compute $F_1'(0)$. Thus an untraviolet cutoff is unnecessary and the integral can be performed as a function of $m_5^2 = m_6^2 = \lambda^2$.

Our result for the contribution to $F_1'(0)$ from the corner graph along with the analytic result for the asymptotic region ($\lambda << m$) given by Soto is shown in Figure 5. After correcting for the sign discrepancy the two curves become parallel in the asymptotic ($\lambda \to 0$) region rather than joining. The expectation that the sum of corner plus self-energy contributions are finite for $\lambda \to 0$ is confirmed in Figure 6.

In order to determine the constant term in the corner graph contribution, we have constrained the coefficients of the $\log^2 \lambda^{-2}$ and $\log \lambda^{-2}$ terms to be the negative of Soto's and performed several types of least-square fits to the results of the numerical integration using "background" terms multiplying $\sqrt{\lambda^2}$, $\sqrt{\lambda^2}\log\lambda^2$ and $\lambda^2 \log \lambda^2$. The resulting constant term from the corner graph, shown in Figure 1, column 2, differs substantially from the constant term in Soto's expression. A consistent value for the sum of self-energy and corner contributions for $\lambda^2 \to 0$ can be obtained directly from Figure 6 without any detailed curve fitting or knowledge of the infrared divergent behavior of the individual contributions.

As another check on the calculation we have also calculated the corner graph contribution using <u>intermediate renormalization.</u> In this method the subtraction term is computed as in Eq. (4.17) but the internal vertex is computed with its fermion and photon legs all on the $m = 0$ mass shell. The subtraction term can be obtained immediately from the unrenormalized amplitude by replacing $k_1, k_2 \to 0$, $B_{14} \to 0$, and keeping only the terms in U, D, k_3, k_4 which are of lowest order in z_1, z_2, or z_5. A complete discussion of intermediate renormalization in Feynman parameter space is given in Ref. (24).

The correction term which compensates for the error made in renormalizing at $m = 0$ is simply

$$(2) \left. \frac{dF_1^{(2)}}{dq^2} \right|_0 \times \left[\Lambda^{(2)}(0,0,0) - \Lambda^{(2)}(m,m,0) \right] \tag{4.19}$$

where the first factor is defined in Eq. (3.2) and

$$\Lambda^{(2)}(0,0,0) - \Lambda^{(2)}(m,m,0) = \frac{\alpha}{2\pi} \int_0^1 dz\, z \left[\frac{1}{z + \lambda^2(1-z)} - \frac{(-2+2z+z^2)}{z^2 + \lambda^2(1-z)} + \log \frac{z^2+\lambda^2(1-z)}{z+\lambda^2(1-z)} \right]$$

$$\xrightarrow[\lambda \ll m]{} \frac{\alpha}{\pi} \left[\log \frac{m}{\lambda} - \frac{7}{8} \right] \tag{4.20}$$

is calculated from the coefficient of γ_α of the unrenormalized vertex in second order. The numerical results are consistent with that obtained using renormalization on the mass shell.

As a final check on the corner graph contribution to $F_1'(0)$ we have also projected out the contribution of this graph to $F_2(0)$, the anomalous magnetic moment of the electron. Since the same parametric functions that enter F_1 also enter F_2, since the same method of internal renormalization is used, and since the same integration program is used, this is a reasonably good check on the calculation. The result shown in Figure 7 is in excellent agreement with Petermann's result[18]. The logarithmic dependence on the photon mass, which cancels when the contributions of all fourth order graphs to $F_2(0)$ are added, arises from the integration region $z_1, z_2 \sim 0$. The choice of variables

$$\begin{aligned} z_1 &= vu \\ z_2 &= v(1-u) \\ dz_1 dz_2 &= v\,dv\,du \qquad (0 < u < 1) \end{aligned} \tag{4.21}$$

improves the integration efficiency since there is slow dependence of the integrand on u. Similar variable changes were made in all of the numerical calculations in order to check consistency and improve the integration efficiency.

V. THE LADDER AND CROSSED LADDER GRAPHS

The two remaining contributions to the slope of the Dirac form factor in fourth order are shown in Figures Ia and Ie. The sum of the ladder and crossed ladder contributions is infrared convergent and it is convenient to discuss them together.

The calculation of the crossed ladder contribution is quite easy since there is no internal ultraviolet divergence. The method of the previous section can again be used except that for this graph, no internal renormalization subtraction need be made. The result is shown in Figure 8 and again, apart from an overall sign, agreement is found with the log λ^{-2} term in Soto's expression. However, as shown in Figure 1, we disagree slightly with Soto in the finite (non-infrared) term. We have also calculated the contribution of this graph to $F_2(0)$ and have again found excellent agreement with Petermann's result.

The calculation of the ladder graph contribution is nearly identical to that of the corner graph. The internal vertex subtraction is carried out in the same way and in this case we find complete agreement with (the negative of) Soto's result. The comparison is shown in Figure 9. The sum of ladder plus crossed graph contributions is shown in Figure 10.

VI. CONCLUSION

The total contribution to the slope of the Dirac form factor in fourth order is given in Eq. (2.5). The corresponding contribution to the $nS_{\frac{1}{2}} - nP_{\frac{1}{2}}$ level splitting is 0.45 ± 0.07 MHz $\times [Z^4(2/n)^3]$, an increase of $[0.35 \pm 0.07$ MHz$]$ $\times [Z^4(2/n)^3]$ over the previous contributions[2,3,6]. Our result for the fourth order corner graph, which is the primary source of the revision, has been confirmed by a new partially-analytic and partially numeric calculation by de Rafael, Lautrup and Petermann[25]. It would be desirable, however, to have a completely analytic calculation of the F_1' contribution in order to eliminate the errors limits introduced by the numerical calculations. A complete calculation of the order $\alpha(Z\alpha)^6 m$ contribution to the Lamb shift will also be required in order to obtain a theoretical prediction with a limit of error several times smaller than the errors quoted for the experimental results.

The reconciliation of the QED calculations with the Lamb shift experiments (see Table I) is very gratifying. At the present time not one of the sensitive QED comparisons of theory and experiment is in serious disagreement[3].

Unlike the colliding-beam, $(g-2)_\mu$ and hyperfine splitting measurements, the Lamb shift measurements are not particularly useful for limiting high-momentum transfer modifications of QED,[26] although the current agreement with experiment does rule out speculations of the type discussed by Barrett et al.[27] (long charge tails on the nucleus) and Yennie and Farley[28] (low mass scalar particle exchange). It is interesting to note that the magnitude and Z and n dependence of the proposed modifications of the hadronic contribution to the Lamb shift are the same as those caused by the reevaluation of the fourth order contributions discussed in this paper.

ACKNOWLEDGEMENTS

We wish to thank our colleagues at SLAC especially S. Drell and J. Primack for their encouragement and helpful discussions. We also wish to thank Professor D. R. Yennie for several stimulating discussions and helpful suggestions. The cooperation of the SLAC Computation Center is also deeply appreciated. We also acknowledge our great debt to A. C. Hearn for making his algebraic computation program REDUCE available to us, and to G. Sheppey for the development of his numerical integration program.

REFERENCES

1. W. E. Lamb, Jr. and R. E. Retherford, Phys. Rev. 86, 1014 (1952) and references therein. S. Triebwasser, E. S. Dayhoff and W. E. Lamb, Jr., Phys. Rev. 89, 98 and 106 (1953).
2. H. A. Bethe, Phys. Rev. 72, 339 (1947).
3. S. J. Brodsky, Status of Quantum Electrodynamics, Invited talk presented at the 1969 International Symposium on Electron and Photon Interactions at High Energies, Liverpool, England, September 14 to 20, 1969, SLAC-PUB-676.
4. R. T. Robiscoe and T. W. Shyn, unpublished. See B. Taylor, W. Parker, and D. Langenberg, Rev. Mod. Phys. 41, 375 (1969). B. L. Cosens, Phys. Rev. 173, 49 (1968).
5. See the references for Table I(b)
6. S. L. Kaufman, W. E. Lamb, K. R. Lea and M. Leventhal, Phys. Rev. Letters 22, 507 (1969). T. W. Shyn, W. L. Williams, R. T. Robiscoe and T. Rebane, Phys. Rev. Letters 22, 1273 (1969). T. V. Vorburger and B. L. Cosens, Phys. Rev. Letters 23, 1273 (1969).
7. A. J. Layzer, Phys. Rev. Letters 4, 580 (1960).
8. R. Karplus, A. Klein and J. Schwinger, Phys. Rev. 86, 288 (1952).
9. G. W. Erickson and D. R. Yennie, Ann. Phys. (N.Y.) 35, 271 (1965). G. W. Erickson and D. R. Yennie, Ann. Phys. (N.Y.) 35, 447 (1965).
10. E. E. Salpeter, Phys. Rev. 87, 328 (1952).
11. H. Grotch and D. R. Yennie, Rev. Mod. Phys. 41, 350 (1969).
12. S. J. Weneser, R. Bersohn and N. Kroll, Phys. Rev. 91, 1257 (1953). M. F. Soto, Jr., Phys. Rev. Letters 17, 1153 (1966). This is the only analytic calculation of the fourth order contribution. It was previously estimated by Weneser, Bersohn and Kroll (Ref.12).
13. T. Appelquist and S. J. Brodsky, Phys. Rev. Letters 24, 562 (1970).

14. R. Mills and N. Kroll, Phys. Rev. 98, 1489 (1955).

15. We use the notation and conventions of J. D. Bjorken and S. D. Drell, Relativistic Quantum Mechanics, McGraw-Hill, Inc. (1964). Note that a form factor which falls for space-like q^2 $(dF_1(0)/dq^2 > 0)$ reduces the binding of s-states and therefore contributes a positive contribution to the Lamb shift. A derivation of Eq. (2.2) can be found in D. R. Yennie and G. W. Erickson, Ref. 9.

16. It can be seen quite easily that the slope of the Dirac form factor in order α^2 will be convergent in the infrared by using the well-known result of Yennie, Frautschi and Suura (Ann. of Phys. 13, 379 (1961)) that the logarithmic dependence on the photon mass can be regrouped into a multiplicative exponential factor. A careful analysis shows that the renormalized vertex $\tilde{\Gamma}_\mu(p,p')$ can be written in the form

$$\tilde{\Gamma}_\mu(p,p') = e^B \Gamma_{\mu\, NIR}$$

$$= \gamma_\mu + B\gamma_\mu + \Lambda_\mu^{(2)} + \tfrac{1}{2}(B)^2\gamma_\mu + B\Lambda_\mu^{(2)} + \Lambda_\mu^{(4)} + O(\alpha^3)$$

where B contains all the logarithmic dependence on the photon mass and $\Lambda_\mu^{(2)}$ and $\Lambda_\mu^{(4)}$ are finite when the photon mass is set equal to zero. Since both B and the F_1 part of $\Lambda_\mu^{(n)}$ vanish like q^2 when $q^2 \to 0$, we see that the fourth order Dirac form factor to order q^2 is convergent in the infrared. We wish to thank Professor D. R. Yennie for discussions on this point. It must also be shown that the photon mass device leads to the same non-infrared remainder as the actual regularization procedure from binding corrections. This is in fact what has been established by Mills and Kroll, Ref. 14.

17. R. Karplus and N. M. Kroll, Phys. Rev. 77, 536 (1950).

18. A. Petermann, Helv. Phys. Acta 30, 407 (1957).

19. A. C. Hearn, Report No. ITP-247, Stanford University, Stanford, California (1968).

20. N. Nakanishi, Prog. Theor. Phys. Suppl. 18, 1 (1961). N. Nambu, Nuovo Cimento 6, 1064 (1957). K. Symanzik, Prog. Theor. Phys. 20, 690 (1958).

21. J. Aldins, S. J. Brodsky, A. J. Dufner, and T. Kinoshita, Phys. Rev. Letters 23, 441 (1969) and to be published.

22. This is simply the spectral representation for the photon propagator to first order in α. G. Källén, Helv. Phys. Acta 25, 417 (1952).

23. J. M. Jauch and F. Rohrlich, The Theory of Photons and Electrons, Addison-Wesley, Inc. (1955). The result for $\lambda^2 = 0$ in Eq. 9-24 which is infrared divergent contains a sign error in one term. The subtraction constant B, which contributes to electron wave function renormalization, is also infrared divergent in the limit $\lambda^2 \to 0$. It is, of course, exactly cancelled due to the Ward identity once vertex and external line wave function renormalization constants are included.

24. T. Appelquist, Ann. Phys. (N.Y.) 54, 27 (1969).

25. E. de Rafael, B. Lautrup, A. Petermann, Th-1140-CERN.

26. J. Kraus, Nucl. Phys. B11, 588 (1969).

27. R. C. Barrett, S. J. Brodsky, G. W. Erickson, M. M. Goldhaber, Phys. Rev. 166, 1587 (1968).

28. See D.R. Yennie, Proc. of the Int. Symposium on Electron and Photon Interactions at High Energies, SLAC, Stanford, Calif. 1967.

TABLE CAPTIONS

Table I The Lamb shift in Hydrogenic Atoms (in MHz). The experimental results for H and D are from Refs. (1-3). Robiscoe's and Cosen's values include a correction for the non-Maxwellian velicity distribution of the atoms in the beam[4]. (R. Robiscoe and T. W. Shyn, private communication. See B. N. Taylor et al., Ref. (4), note added in proof.) The values for $\mathscr{L}_{\rm exp}$ listed in parenthesis are computed from experimental measurements of the large interval "$\Delta E - \mathscr{L}$" $= \Delta E(2P_{\frac{3}{2}} - 2S_{\frac{1}{2}})$ and the theoretical fine structure (see Table III). The "old" theoretical values are from B. N. Taylor et al. (Ref. 2). The revised theory corresponds to the corrected result for the fourth order contributions discussed in this paper. We use the conventions of B. N. Taylor et al., Ref. (4), and take the limit of error (L.E.) to be three standard deviations.

Table II Tabulation of the theoretical contributions to the Lamb interval $\mathscr{L} = \Delta E(2S_{\frac{1}{2}} - 2P_{\frac{1}{2}})$ in H. References to the various entries may be found in G. W. Erickson and D. R. Yennie (Ref. 9) and B. N. Taylor et al. (Ref. 4). The dependence on nuclear charge is retained to distinguish binding and radiative corrections. Column one gives the former theoretical result which includes the order $\alpha^2(Z\alpha)^4 m$ contribution to the energy shift from the slope of the Dirac form factor in fourth order as given by M. Soto (Ref. 12). The revised theory, corresponding to the corrected value for this contribution as given by Eqs. (2.5) and (2.2), is listed in column two. Note that fourth order contributions to the Lamb interval also arise from the fourth order anomalous moment and vacuum polarization corrections.

Table III Comparison of the results of this calculation and that of Ref. (12) for the Feynman graph contributions to $a_4 = m^2 d\, F_1/dq^2\ (q^2=0)/(\alpha^2/\pi^2)$. The corner and self energy graph results include the contribution of mirror graphs. The infrared behavior is expressed in terms of a photon-mass parametrization for $\lambda^2 \ll m^2$. The infrared convergent ladder plus cross contributions (0.68 ± 0.04) as well as the corner plus self energy contribution (-0.23 ± 0.03) could be obtained without knowledge of the infrared divergent behavior of the individual graphs, which were, however, found to be consistent with the negative of the asymptotic behavior ($\lambda^2 \ll m^2$) given in Ref. (12). The individual non-infrared remainders given in the last column were determined from fits with the logarithmic terms constrained to those values plus "background" terms multiplying $\sqrt{\lambda^2}$, $\sqrt{\lambda^2} \log \lambda^2$, and $\lambda^2 \log \lambda^2$.

FIGURE CAPTIONS

1. Feynman diagrams for the fourth order vertex of the electron required to compute the anomalous magnetic moment $F_2(0)$ and the slope $F_1'(0)$.

2. Contribution to the slope of the Dirac form factor in fourth order from fermion self energy insertions in the second order vertex (Figure Id). The solid curve is the result of numerical calculation for various λ^2 (in units of the electron mass squared). The results of this calculation agree asymptotically with Soto's analytic result for $\lambda \to 0$ (dashed curve) except for over-all sign. The top graph gives the difference between the two curves. The error bars represent approximately 1σ in the numerical integration.

3. REDUCE program for computation of the corner graph contribution (Figure 1b) to the slope of the fourth order Dirac form factor. The output of the program is the integrand for five dimensional integration shown in Figure 4. The REDUCE input[19] is in the form of statements beginning with instruction keywords "LET", "MATCH", etc. and ending with semicolons. The "SM X"; (simplify) instruction causes the algebraic simplification (and the taking of $\frac{1}{4}$ trace) of X according to the substitutions defined by previous LET and MATCH statements. The label keywords "VECTOR" and "INDEX" define four vectors and contracted indices, respectively. The quantity G(L, P) represents $\gamma \cdot p$ where γ_μ is the Dirac matrix for fermion L. Other conventions not obvious from context are defined in the non-operational "COMMENT" statements. The constructed program implements the steps outlined in Eqs. (4.1 - 4.15).

4. Fortran program for the numerical evaluation of the renormalized integrand for the five dimensional integration of the corner graph contribution (Figure 1b) to the slope of the Dirac form factor in fourth order. The definitions of the various auxiliary variables U, D, B_{ab}, etc., as determined from Eqs. (4.9 - 4.11), are given in terms of the Feynman integration parameters z_1, z_2, ... z_5. The integrand is renormalized using Eq. (4.17).

5. Numerical results for the corner graph contribution to $F_1'(0)$ as a function of photon mass λ. The dashed curve is the negative of Soto's analytic result for the asymptotic region $\lambda \to 0$. The top graph indicates that the two curves become parallel in the asymptotic region rather than joining. This is the major source of numerical discrepancy between the results of the two calculations.

6. Sum of corner plus self energy contributions Figure (1b, 1d) to $F_1'(0)$ in fourth order as a function of photon mass λ^2. The expectation that this sum of contributions (Figures 1b and 1d) is finite in the infrared is confirmed. The contribution $(-0.23 \pm 0.03)\ (\frac{\alpha}{\pi})^2$ can be obtained without any knowledge of the infrared divergent behavior of the individual contributions.

7. Numerical contribution to the fourth order magnetic moment of the electron from the corner diagram (Figure 1b) as a function of photon mass. The dashed line is Petermann's result (Ref. 18), $F_2^{1b}(0) = [\frac{1}{2} \ln \lambda^{-2} - 0.564]\ \frac{\alpha^2}{\pi^2}$ derived for $\lambda \to 0$. As is the case for $F_1'(0)$, the infrared divergence is cancelled by the self-energy contribution (Figure 1d).

8. Numerical contribution to $F_1'(0)$ from the crossed diagram (Figure 1a) as a function of photon mass λ. The dashed curve is the negative of Soto's analytic result for $\lambda \to 0$. The top graph shows that the two curves become parallel in the asymptotic region, disagreeing slightly in the value of the non-infrared remainder.

9. Numerical contribution to $F_1'(0)$ from the ladder diagram (Figure 1e) as a function of photon mass λ. The dashed curve is the negative of Soto's analytic result for the asymptotic region $\lambda \to 0$. Within errors, the two curves are in good agreement as $\lambda \to 0$.

10. Sum of ladder plus crossed diagram (Figures 1a and 1d) contributions to $F_1'(0)$ as a function of photon mass λ^{-2}. The combined contribution $(0.68 \pm .04)\left(\frac{\alpha}{\pi}\right)^2$ to Eq. (2.5) can be obtained without any knowledge of the infrared divergent behavior of the individual contributions.

TABLE I(a)

THE LAMB SHIFT IN HYDROGENIC ATOMS (in MHz)

Reference	$\mathscr{L}_{exp}$ ($\pm 1\sigma$)	(Old) Theory ($\pm$ L.E.)	(Old) Exp-Th ($\pm 1\sigma$)	Revised Theory ($\pm$ L.E.)	Revised Exp-Th ($\pm 1\sigma$)
H (n = 2)		1057.56 ± 0.09		1057.91 ± 0.16	
Triebwasser, Dayhoff, Lamb (1953)	1057.77 ± 0.06		0.21 ± 0.07		- 0.14 ± 0.08
Robiscoe (Revised, 1969)	1057.90 ± 0.06		0.34 ± 0.07		- 0.01 ± 0.08
Kaufman, Lea, Leventhal, Lamb (1968) [$(\Delta E-\mathscr{L})_{exp} = 9911.38 \pm 0.03$]	(1057.65 ± 0.05)		0.09 ± 0.06		- 0.26 ± 0.07
Shyn, Williams, Robiscoe, Rebane (1969) [$(\Delta E-\mathscr{L})_{exp} = 9911.25 \pm 0.06$]	(1057.78 ± 0.07)		0.22 ± 0.08		- 0.13 ± 0.09
Cosens and Vorburger (1969) [$(\Delta E-\mathscr{L})_{exp} = 9911.17 \pm 0.04$]	(1057.86 ± 0.06)		0.30 ± 0.07		- 0.05 ± 0.08
D (n = 2)		1058.82 ± 0.15		1059.17 ± 0.22	
Triebwasser, Dayhoff, Lamb (1953)	1059.00 ± 0.06		0.18 ± 0.08		- 0.17 ± 0.09
Cosens (Revised, 1969)	1059.28 ± 0.06		0.46 ± 0.08		+ 0.11 ± 0.09

TABLE I(b)

LAMB SHIFT IN OTHER HYDROGENIC ATOMS

Reference	$\mathscr{L}_{exp}$ (± 1σ)	Old Theory (± L.E.)	Old Exp-Th(± 1σ)	Revised Theory(± L.E.)	Revised Exp-Th (± 1σ)
He^{+} (n = 2)		14038.9 ± 4.1		14044.5 ± 5.2	
Lipworth, Novick (1957)[a]	14040.2 ± 1.8		1.3 ± 2.2		- 4.3 ± 2.5
Narasimham (1968)[b, c]	14045.4 ± 1.2		6.5 ± 1.8		1.0 ± 2.1
He^{+} (n = 3)		4182.7 ± 1.2		4184.4 ± 1.5	
Mader, Leventhal (1969)[d, c]	4182.4 ± 1.0		-0.3 ± 1.1		- 2.0 ± 1.1
Mader, Leventhal (1969)[c]	(4184.0 ± 0.6)		1.3 ± 0.7		- 0.4 ± 0.8
[ΔE-$\mathscr{L}$= 47843.8 ± 0.5]					
He^{+} (n = 4)		1768.3 ± 0.5		1769.0 ± 0.6	
Hatfield, Hughes (1968)[e]	1776.0 ± 7.5		-2.3 ± 7.5		- 3.0 ± 7.5
Jacobs, Lea, Lamb (1969)[f, c]	1768.0 ± 5.0		-0.3 ± 5.0		- 1.0 ± 5.0
Jacobs, Lea, Lamb (1969)[c]	(1769.4 ± 1.2)		+1.1 ± 1.3		0.4 ± 1.3
[ΔE-$\mathscr{L}$= 20179.7 ± 1.2]					
Li^{++} (n = 2)		62743.0 ± 45.0		62771.0 ± 50.0	
Fan, Garcia-Munoz, Sellin (1967)[g]	63031.0 ± 327.0		288.0 ± 333.0		260.0 ± 333.0

References for Table Ib

a) E. Lipworth and R. Novick, Phys. Rev. 108, 1434 (1957).

b) M. A. Narasimham, Ph.D. Thesis, University of Colorado, 1968 (unpublished).

c) Private communication reported by B. N. Taylor, W. H. Parker, D. N. Langenberg.

d) D. Mader and M. Leventhal, International Conference on Atomic Physics, New York University (1968).

e) L. L. Hatfield and R. N. Hughes, Phys. Rev. 156, 102 (1967).

f) R. R. Jacobs, K. R. Lea, W. E. Lamb, Jr., Bull. Am. Phys. Soc. 14, 525 (1969).

g) C. Y. Fan, M. Garcia-Munoz and I. A. Sellin, Phys. Rev. 161, 6 (1967).

TABLE II

VARIOUS CONTRIBUTIONS TO THE LAMB SHIFT IN H (n = 2)

DESCRIPTION	ORDER	OLD TABULATION	NEW TABULATION
2^{nd} ORDER — SELF-ENERGY	$\alpha(Z\alpha)^4 m\{\log Z\alpha, 1\}$	1079.32 ± 0.02	1079.32 ± 0.02
2^{nd} ORDER — VAC. POL.	$\alpha(Z\alpha)^4 m$	-27.13	-27.13
2^{nd} ORDER — REMAINDER	$\alpha(Z\alpha)^5 m$	7.14	7.14
	$\alpha(Z\alpha)^6 m\{\log^2 Z\alpha, \log Z\alpha, 1\}$	-0.38 ± 0.04	-0.38 ± 0.04
4^{th} ORDER — SELF-ENERGY	$\alpha^2(Z\alpha)^4 m \; F_1'(0)$	0.10	0.45 ± 0.07
	$\alpha^2(Z\alpha)^4 m \; F_2(0)$	-0.10	-0.10
	$\alpha^2(Z\alpha)^5 m$	± 0.02	± 0.02
4^{th} ORDER — VAC. POL.	$\alpha^2(Z\alpha)^4 m$	-0.24	-0.24
REDUCED MASS CORRECTIONS	$\alpha(Z\alpha)\frac{m}{M} m\{\log Z\alpha, 1\}$	-1.64	-1.64
RECOIL	$(Z\alpha)^5 \frac{m}{M} m\{\log Z\alpha, 1\}$	0.36 ± 0.01	0.36 ± 0.01
PROTON SIZE	$(Z\alpha)^4 (mR_N)^2 m$	0.13	0.13
	$\mathscr{L} = \Delta E(2S_{\frac{1}{2}} - 2P_{\frac{1}{2}})$	1057.56 ± 0.08	1057.91 ± 0.16 (L.E.)
$\alpha^{-1} = 137.03608$	$\Delta E(2P_{\frac{3}{2}} - 2S_{\frac{1}{2}})$	9911.47 ± 0.15	9911.12 ± 0.22 (L.E.)
	$\Delta E(2P_{\frac{3}{2}} - 2P_{\frac{1}{2}})$	10969.03 ± 0.12	10969.03 ± 0.12 (L.E.)

TABLE III

		Soto	This Calculation
a_{cross}	(Fig. 1a)	$\frac{13}{36}\log\lambda^{-2} - 2.314$	$-\frac{13}{36}\log\lambda^{-2} + 2.37 \pm 0.02$
a_{corner}	(Fig. 1b)	$-\frac{1}{12}\log^2\lambda^{-2} + \frac{1}{72}\log\lambda^{-2} + 2.432$	$\frac{1}{12}\log^2\lambda^{-2} - \frac{1}{72}\log\lambda^{-2} - 1.91 \pm 0.02$
$a_{vac\text{-}pol}$	(Fig. 1c)	$-\ 0.0316$	$+\ 0.0316 \pm 0.0002$
$a_{self\text{-}energy}$	(Fig. 1d)	$\frac{1}{12}\log^2\lambda^{-2} - \frac{1}{72}\log\lambda^{-2} - 1.688$	$-\frac{1}{12}\log^2\lambda^{-2} + \frac{1}{72}\log\lambda^{-2} + 1.68 \pm 0.01$
a_{ladder}	(Fig. 1e)	$-\frac{13}{36}\log\lambda^{-2} + 1.710$	$+\frac{13}{36}\log\lambda^{-2} - 1.69 \pm 0.02$
a_4		0.108	0.48 ± 0.07

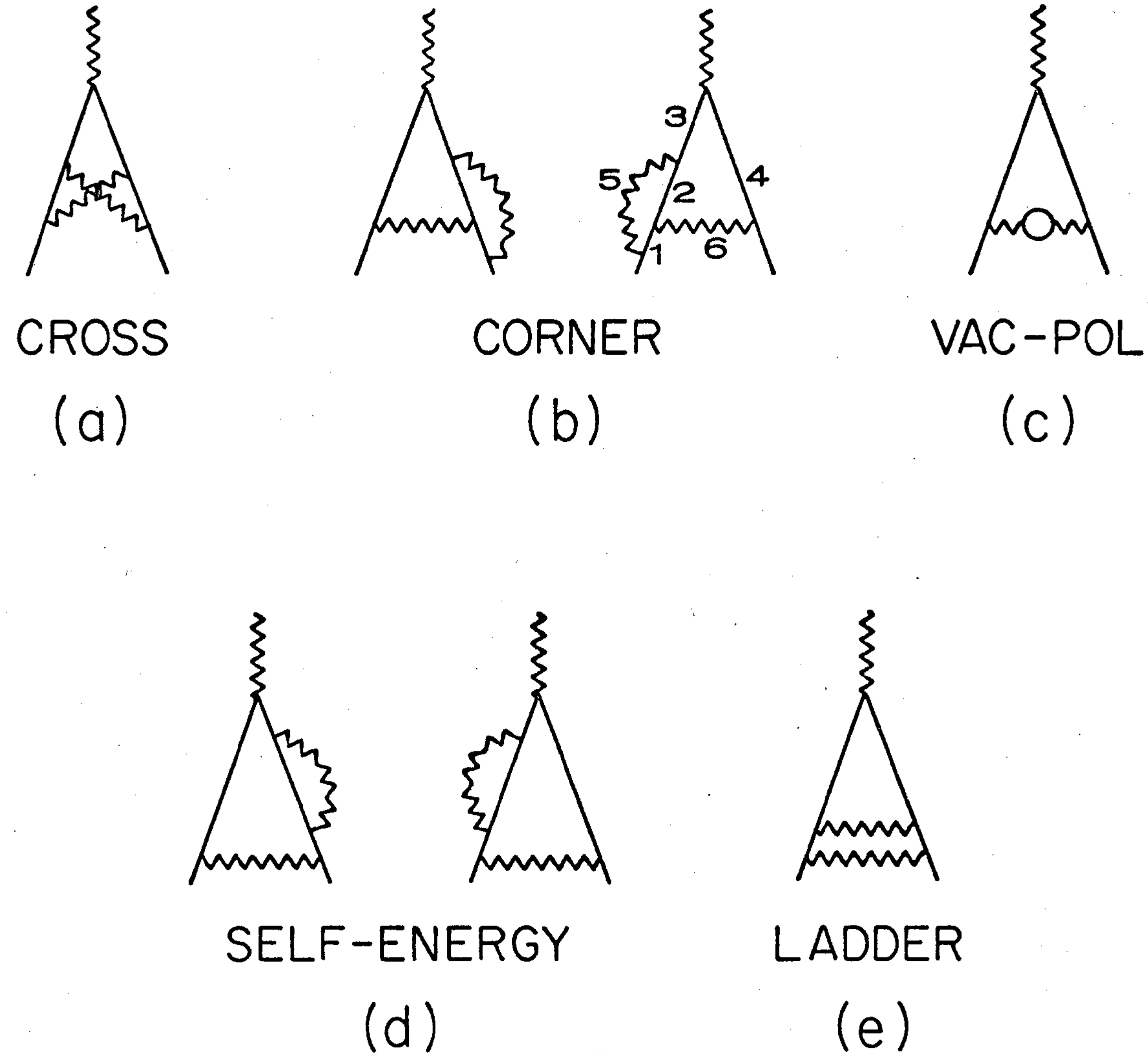

Fig. 1

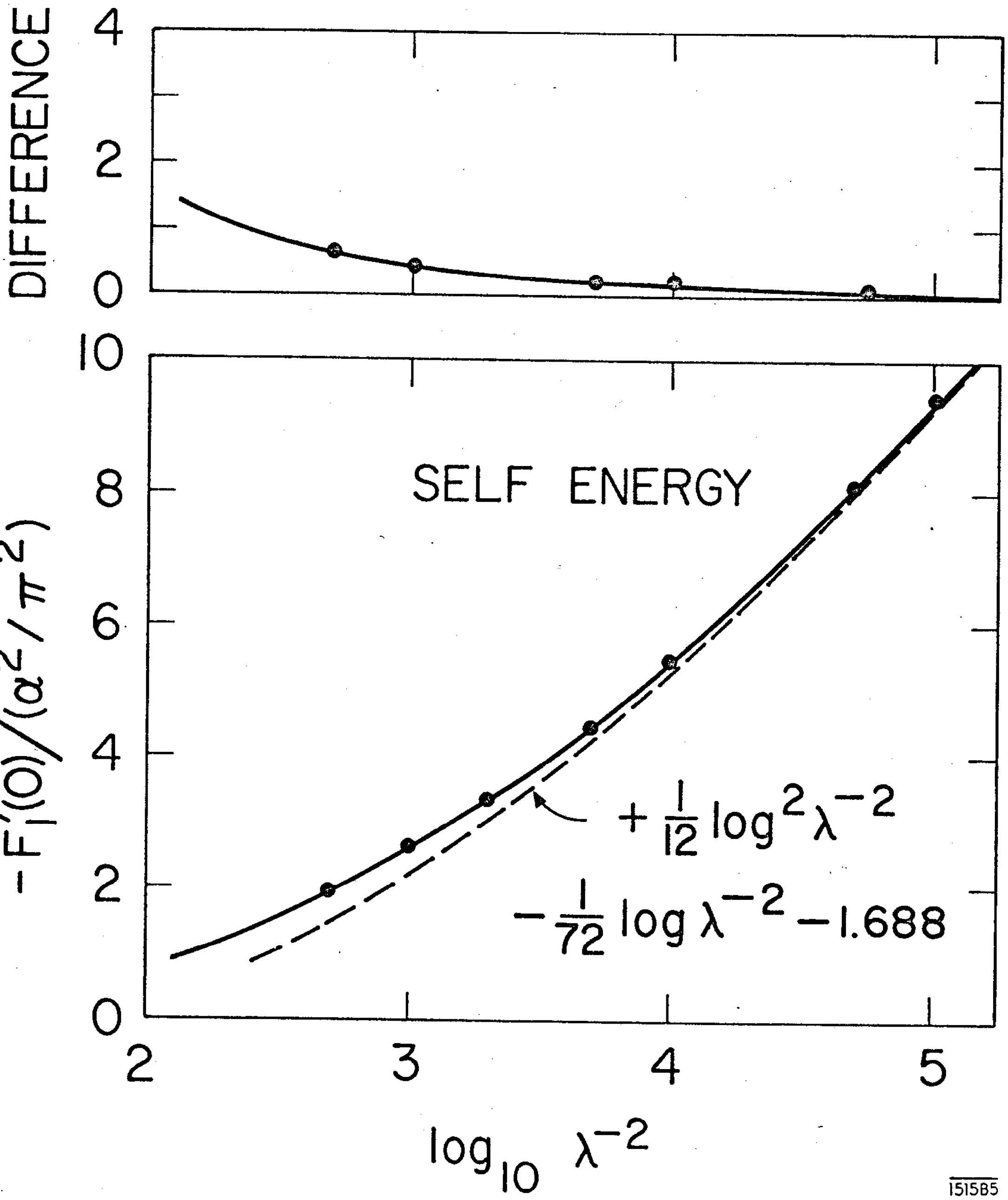

DIFFERENCE
SELF ENERGY
$-F_1'(0)/(\alpha^2/\pi^2)$
$+\frac{1}{12}\log^2\lambda^{-2}$
$-\frac{1}{72}\log\lambda^{-2}-1.688$
$\log_{10}\lambda^{-2}$
1515B5

Fig. 2

```
BEGIN ()
COMMENT  REDUCE PROGRAM TO COMPUTE F1(QS) CONTRIBUTION OF CORNER GRAPH;

COMMENT  THE FOLLOWING NAME 4-VECTORS AND INDICES ;
VECTOR Y1,Y2,Y3,Y4,Q,P;
INDEX LA,SI,MU,RH;
IFLAG;
COMMENT THE EXTERNAL PHOTON 4-MOMENTUM IS 2*Q, Q.Q=Q2=QS/4;
ORDER QS,M2; FACTOR QS,M2,P2;
COMMENT  G(L,P) IS GAMMA.P = P SLASH;
OPERATOR GM,PR1;
RULE GM(P)= G(L,P)+M;
RULE PR1(MU)= (-P2*G(L,MU)+3*M*P.MU)/(4*P2**2);
LET P.Q=0,P.P=P2,P2= M2-QS/4     ,Q.Q=QS/4,M**2=M2;
   LET PR = GM(P-Q)*PR1(MU)*GM(P+Q);
COMMENT TEST PROJECTION OPERATOR FOR F1 FORM FACTOR;
COMMENT   REDUCE COMPUTES 1/4 * TRACE IN SM=SIMPLIFY STEP;
                 SM PR*(G(L,MU,Q)-G(L,Q,MU));
GCDIT;
SM PR*G(L,MU);
NOGCD;
OPERATOR STR;
COMMENT  THE FOLLOWING IS THE TRACE STRING FOR THE CORNER GRAPH;
RULE STR(G4,G3,G2,G1)= PR*
G(L,LA)*G4* G(L,MU)*G3     *G(L,SI)*G2*G(L,LA)*G1*G(L,SI);
SM STR(GM(Y4),GM(Y3),GM(Y2),GM(Y1));
OPERATOR FS; SAVEAS FS(Z);
COMMENT THE RESULT IS STORED AS FS(Z), Z IS A DUMMY ARGUMENT;
CLEAR P2;
LET QS = 4*(M2-P2);
COMMENT THE FOLOWING EXPRESS 4-MOMENTUM CONSERVATION;
LET Y3=Y4-2*Q;
LET Y2= Y1+Y4-P-Q;
SM FS(Z);
SAVEAS FS(Z);
VECTOR L1,L2,L3,L4;
LET Y1 = A1*P+B1*Q+S*L1;
LET Y2= A2*P+B2*Q+S*L2;
LET Y4 = A4*P+B4*Q+S*L4;
COMMENT THE FOLLOWING ELIMINATES ODD POWERS OF LOOP MOMENTA IN THE NUM;
MATCH S=0, S**3=0, S**2=S2,S**4=S4;  FACTOR S2,S4;
SM FS(Z); SAVEAS FS(Z);
VECTOR X,Y;  FREE X,Y;
COMMENT     THE FOLLOWING ELIMINATES L.P*L.Q TERMS;
LET S2*P.X*Q.Y=0, S4*P.X*Q.Y=0;
SM FS(Z); SAVEAS FS(Z);
FREE P,Q;
OPERATOR FX;  SAVEAS FX(P,Q);
LET CP**2= P2/4, CQ**2= QS/16;
INDEX QI,PI;
COMMENT  THE FOLLOWING REPLACES P.L*P.L WITH 1/4*P2*L.L;
SM FX(CP*PI,CQ*QI);
OPERATOR FT;
FREE X;  SAVEAS FT(X);
VECTOR U,V; FREE U,V;
COMMENT  THE FOLLOWING IS FOR LOOP INTEGRAL WITH QUARTIC NUMERATOR;
LET S4*X.Y*U.V=C*(4*X.Y*U.V+X.U*Y.V+X.V*Y.U);
SM FT(X);
SAVEAS ANS;
CLEAR QS;
LET P2=M2-QS/4;
COMMENT  FINAL SUBSTITIONS FOR LOOP INTEGRATION;
SM SUB(L1.L2=B12,L1.L3=B13,L1.L4=B14,L2.L3=B23,L3.L4=B34,L2.L4=B24,
   L1.L1=B11,L2.L2=B22,L3.L3=B33,L4.L4=B44,ANS);
FREE Z;
SAVEAS FS(Z);
COMMENT  THE FOLLOWING ARE USED FOR COMPUTATION OF F1(QS) SLOPE AT QS=0;
FACTOR M2TT2,M2TQS,S2TQS,S2TM2;
MATCH M2**2=M2TT2,          M2*QS=M2TQS,  S2*QS=S2TQS,S2*M2=S2TM2;
SM FS(Z);
COMMENT THE FOLLOWING PRODUCES A FORTAN DECK OF THE CORNER GRAPH RESULT;
PFORT CALC;
END;
```

Fig. 3

1515A11

```
      FUNCTION F(Q)
C INTEGRAND FOR FIVE DIMENSIONAL INTEGRATION
C  CONTRIBUTION TO SLOPE OF F1(QS) AT QS=0.
C CORNER GRAPH WITH SUBTRACTION TERM
      IMPLICIT REAL*8 (A-Z)
      DIMENSION Q(5)
C THE FOLLOWING NUMERATOR EXPRESSION WAS PUNCHED AUTCMATICALLY BY REDUCE
      CORNER(QS) =
     1(S2TM2*(8*A1**2*B44-40*A1*A4*B14-12*A1*B44+8*A1*B14-4*A4**2*B11-
     136*A4**2*B14+12*A4*B44+16*A4*B11+84*A4*B14+4*B44-4*B11)+S2TQS*(2
     1*A1*A4*B44+2*A1*A4*B14+2*A1*B44+2*A1*B14+B4**2*B11+B4**2*B14-2*
     1B4*B44*B1-2*B4*B1*B14-2*B4*B11-2*B4*B14-A4**2*B11-A4**2*B14-2*A4
     1*B11-2*A4*B14+2*B44*B1+2*B1*B14)+M2TT2*(-16*A1**2*A4**2+16*A1**2
     1*A4-16*A1**2-16*A1*A4**3+48*A1*A4**2+32*A1+8*A4**3+16*A4**2-40*
     1A4)+M2TQS*(4*A1**2*B4**2-8*A1**2*B4+4*A1**2*A4**2-4*A1**2*A4+8*
     1A1**2+4*A1*B4**2*A4-8*A1*B4**2-8*A1*B4*A4*B1-20*A1*B4*A4+20*A1*
     1B4+4*A1*A4**3-12*A1*A4**2+8*A1*A4*B1+16*A1*A4-20*A1+2*B4**2*A4-8
     1*B4*A4**2*B1+20*B4*A4*B1+4*B4-2*A4**3+20*A4**2*B1+4*A4*B1**2-28*
     1A4*B1+4*A4+12*B1)+8*C*B44*B11-24*C*B44*B14-32*C*B14**2)/(2)
C THE FOLLOWING IS THE CORRESPONDING SUBTRACTION TERM
      CORSUB(QS)=
     1(M2TT2*(8*A4**2*A1**2-32*A4**2*A1+8*A4**2-32*A4*A1**2+128*A4*A1-
     132*A4+8*A1**2-32*A1+8)+M2TQS*(-2*B4**2*A1**2+8*B4**2*A1-2*B4**2+
     14*B4*A1**2-16*B4*A1+4*B4+2*A4**2*A1**2-8*A4**2*A1+2*A4**2+4*A4*
     1A1**2-16*A4*A1+4*A4)+M2TS2*(-4*A4**2*B11+16*A4*B11-4*A1**2*B44+
     116*A1*B44-4*B44-4*B11)+QSTS2*(B4**2*B11-2*B4*B11-A4**2*B11-2*A4*
     1B11)+8*C*B44*B11)/(2)
C  (QS IS A DUMMY ARGUMENT IN ABOVE ARITHMETIC STATEMENT DEFINITIONS)
      L2 = 5.E-5
C L2 IS THE PHOTON MASS SQUARED
       QS=0.
C  INTEGRATION IS OVER Q(I),I=1,5  FROM 0 TO 1
      X = Q(1)
      Y= Q(2)
      V= Q(3)
      U=Q(4)
      Z5=Q(5)
      ZT = X+V+Z5
C THE FOLLOWING CORRESPONDS TO THE THETA FUNCTION CONSTRAINT
      IF (ZT .LT. 1.) GO TO 1
      F=0.
      RETURN
    1 Z6 = 1.-ZT
      Z3 = V*U
      Z4 = V*(1.-U)
      Z1= X*Y
      Z2= X*(1-Y)
C  WRK IS WRCNSKIAN FOR VARIABLE CHANGE
      WRK = V*X
      M2 = 1
      Z14 = Z1+Z4
      Z15 = Z1+Z5
      Z16 = Z1+Z6
      Z45 = Z4+Z5
      Z56 = Z5+Z6
```

Fig. 4

1515A10

```
      Z23 = Z2+Z3
      Z46 = Z4+Z6
      Z12 = Z1+Z2
      Z34 = Z3+Z4
      Z36 =Z3+Z6
      Z2346 = Z23+Z46
      Z1456 = Z14+Z56
      Z1234 = Z14+Z23

C  CORNER GRAPH DEFINITIONS
C DEFINITIONS OF AUXILIARY VARIABLES IN TERMS OF Z'S
      U1 = Z12+Z5
      Z125 = U1
      U4 = Z3+Z46
      U=U1*U4+ Z2*Z15
      WPP = (Z3+Z4)*(Z125*Z6+Z1*(Z2+Z5))+Z5*Z6*(Z1+Z2)+Z1*Z2*Z5
      WQ= Z3*Z4*U1+Z2*Z4*Z5
      DM = (Z1234 + Z56*L2)*U
      A1 =(Z5*Z2346+Z2*Z34)/U
      B1=(-Z5*Z2346+Z2*Z4-Z2*Z3)/U
      A4 = (Z2*Z1+Z6*U1)/U
      B4 = (U1*(Z3+Z36)        +Z2*(Z15+Z5))/U
      B11=Z2346
      B44=U1
      B14=-Z2
      DEN = DM-WPP
      M2TT2= 2*WQ/DEN
      M2TQS=1
      S2TM2=-2*WQ/U**2
      S2TQS=-2*DEN/U**2
      QSTS2=S2TQS
      M2TS2 = S2TM2
      C=WQ*DEN/U**4
      F1= CCRNER(QS)/DEN**2
      FU = F1/8

C SUBTRACTION TERM FOR RENORMALIZATION OF INTERNAL VERTEX ON MASS SHELL
      U=U1*U4
      DM = (Z1234 + Z56*L2)*U
      WPP= Z6*Z34*U1+Z5*Z12*U4
      WQ=Z3*Z4*U1
      A1=Z5/U1
      A4= Z6/U4
      B4=(Z3+Z36)/U4
      B11 = U4
      B44= U1
      B14=0.
      DEN = DM-WPP
      M2TT2= 2*WQ/DEN
      M2TCS=1
      S2TM2=-2*WQ/U**2
      S2TQS=-2*DEN/U**2
      QSTS2=S2TQS
      M2TS2 = S2TM2
      C=WQ*DEN/U**4
      F1S= CORSUB(QS)/DEN**2
      FS  = F1S/8
C   NOTE FACTOR OF 2 INCLUDED FOR MIRROR GRAPH
      F = FU-FS
      F = WRK*F
C  F IS SLOPE OF F1 FORM FACTOR IN UNITS OF (ALPHA/PI))**2
      RETURN
      END
```

1515A9

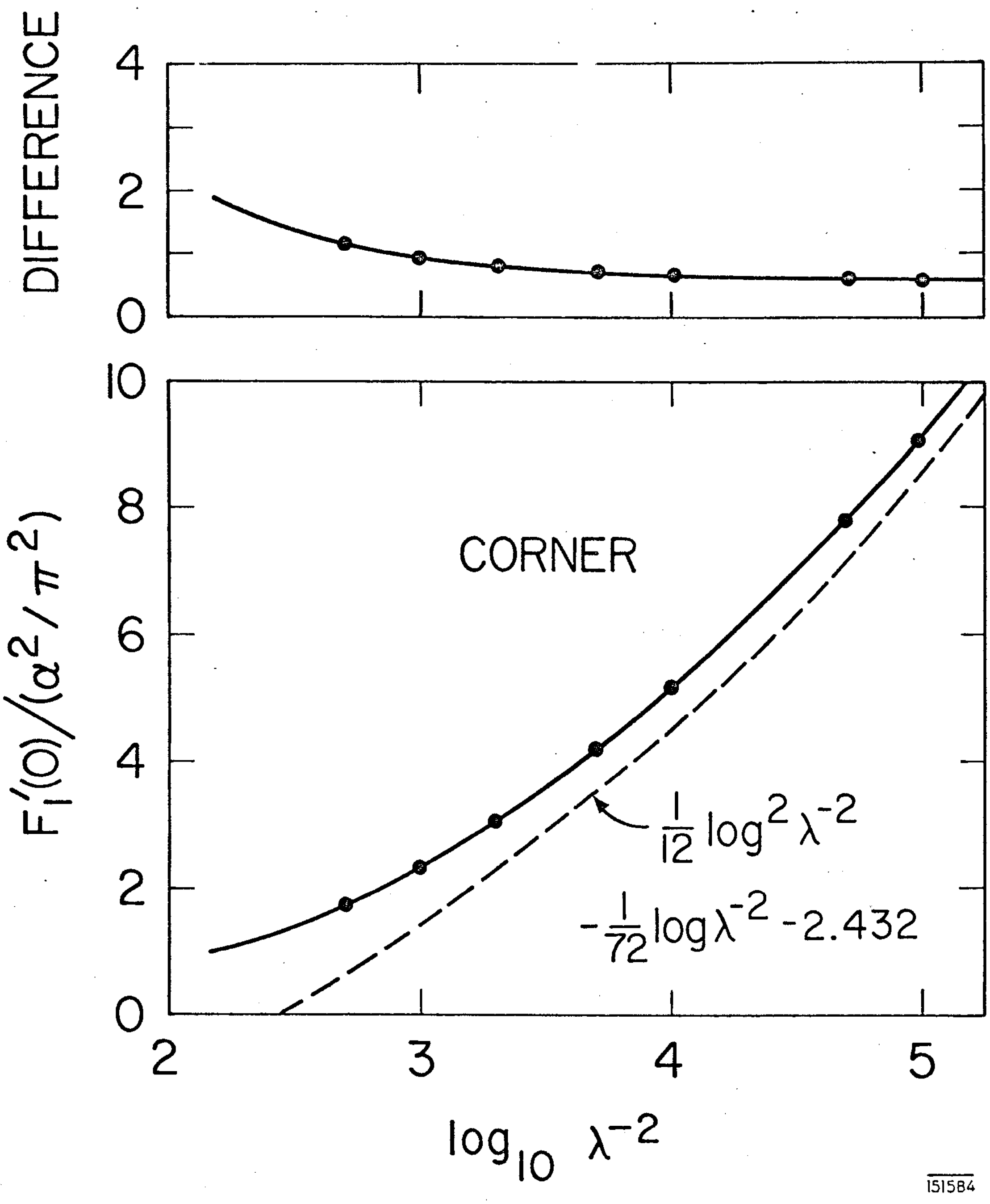
DIFFERENCE
4
2
0
10
8
6
4
2
0
$F_1'(0)/(\alpha^2/\pi^2)$
CORNER
$\frac{1}{12}\log^2\lambda^{-2}$
$-\frac{1}{72}\log\lambda^{-2}-2.432$
2
3
4
5
$\log_{10}\lambda^{-2}$
151584

Fig. 5

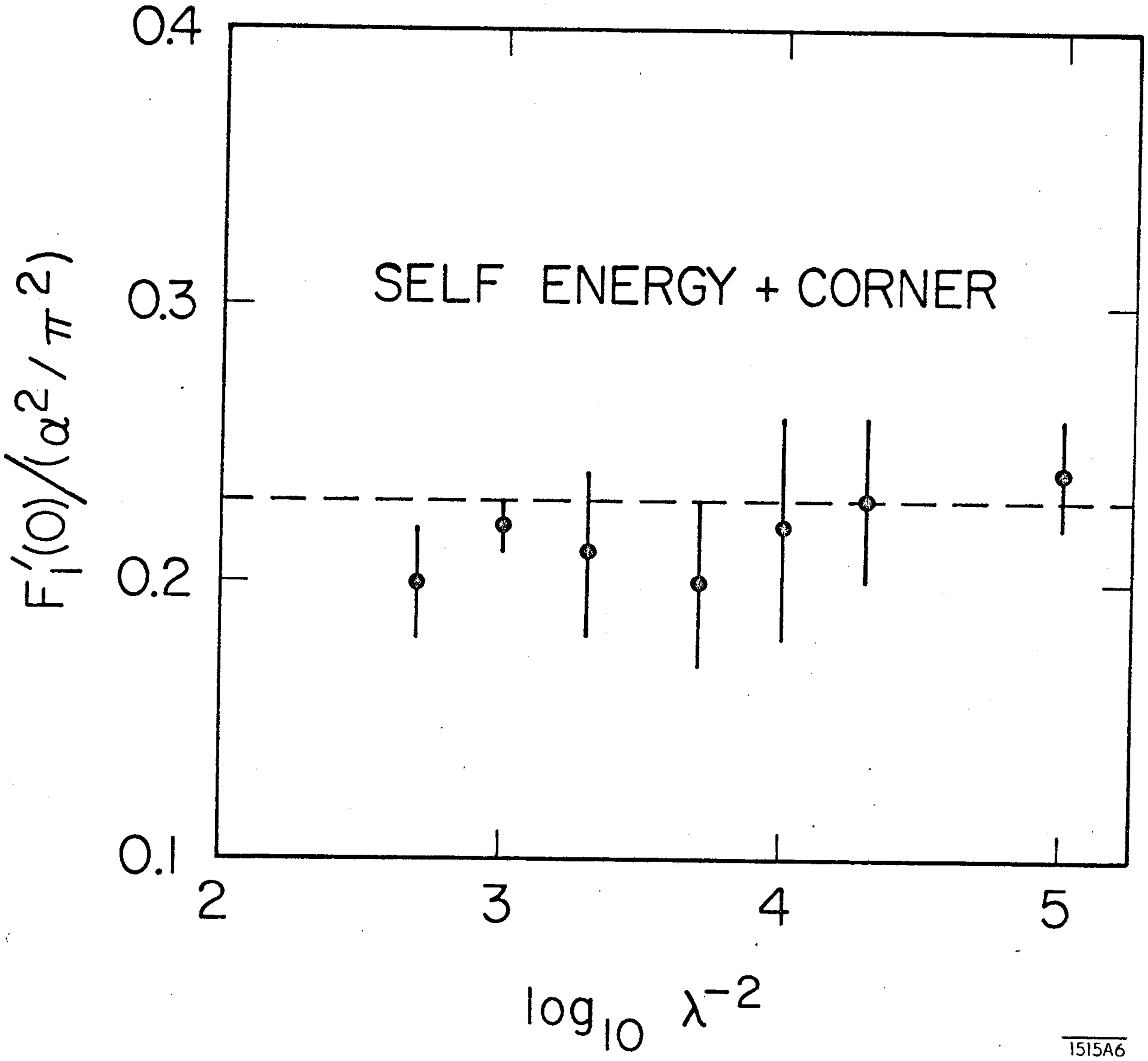

0.4
0.3
0.2
0.1
2
3
4
5
SELF ENERGY + CORNER
$F_1'(0)/(\alpha^2/\pi^2)$
$\log_{10} \lambda^{-2}$
1515A6

Fig. 6

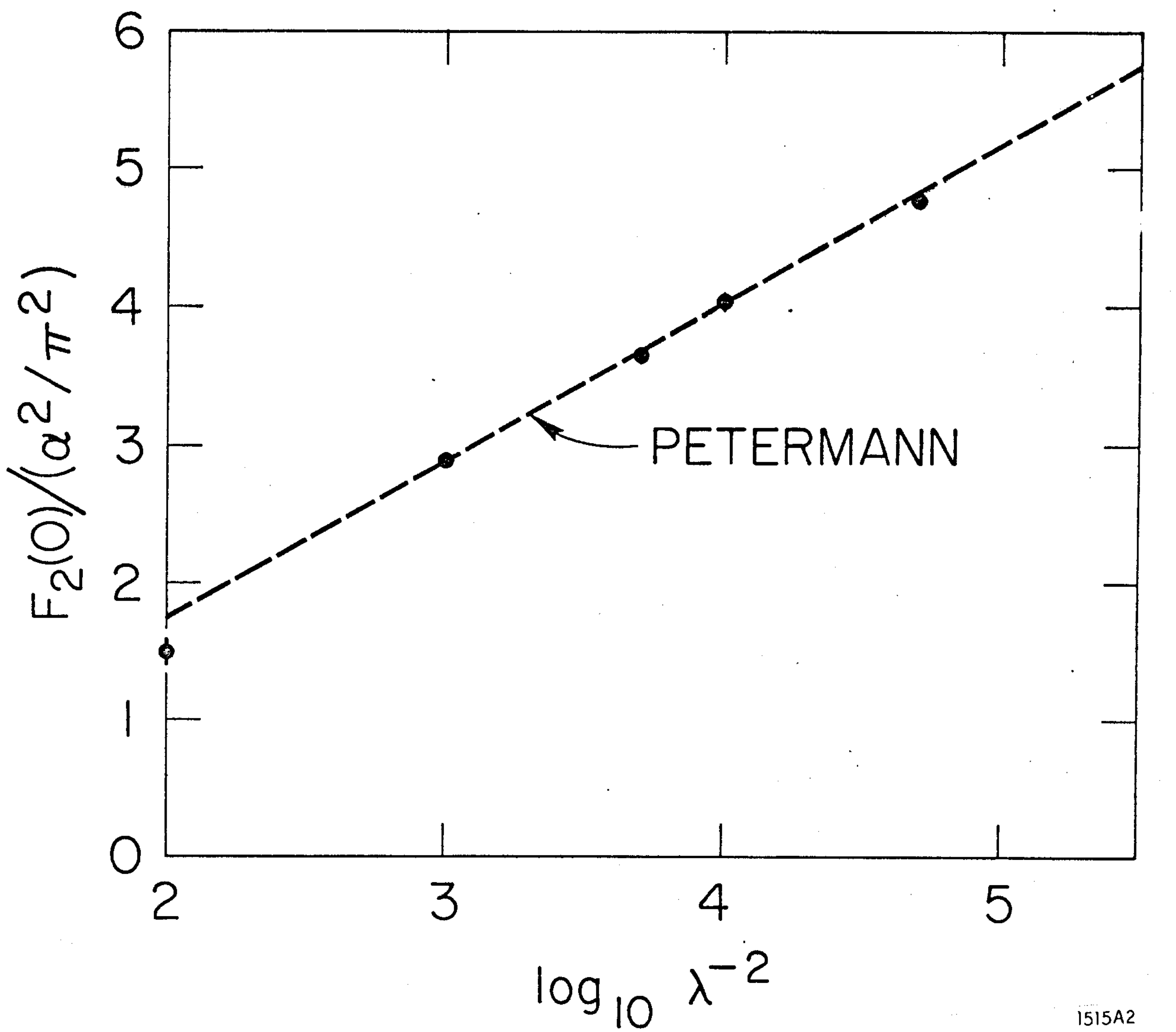

0
1
2
3
4
5
6
2
3
4
5
$F_2(0)/(\alpha^2/\pi^2)$
$\log_{10} \lambda^{-2}$
PETERMANN
1515A2

Fig. 7

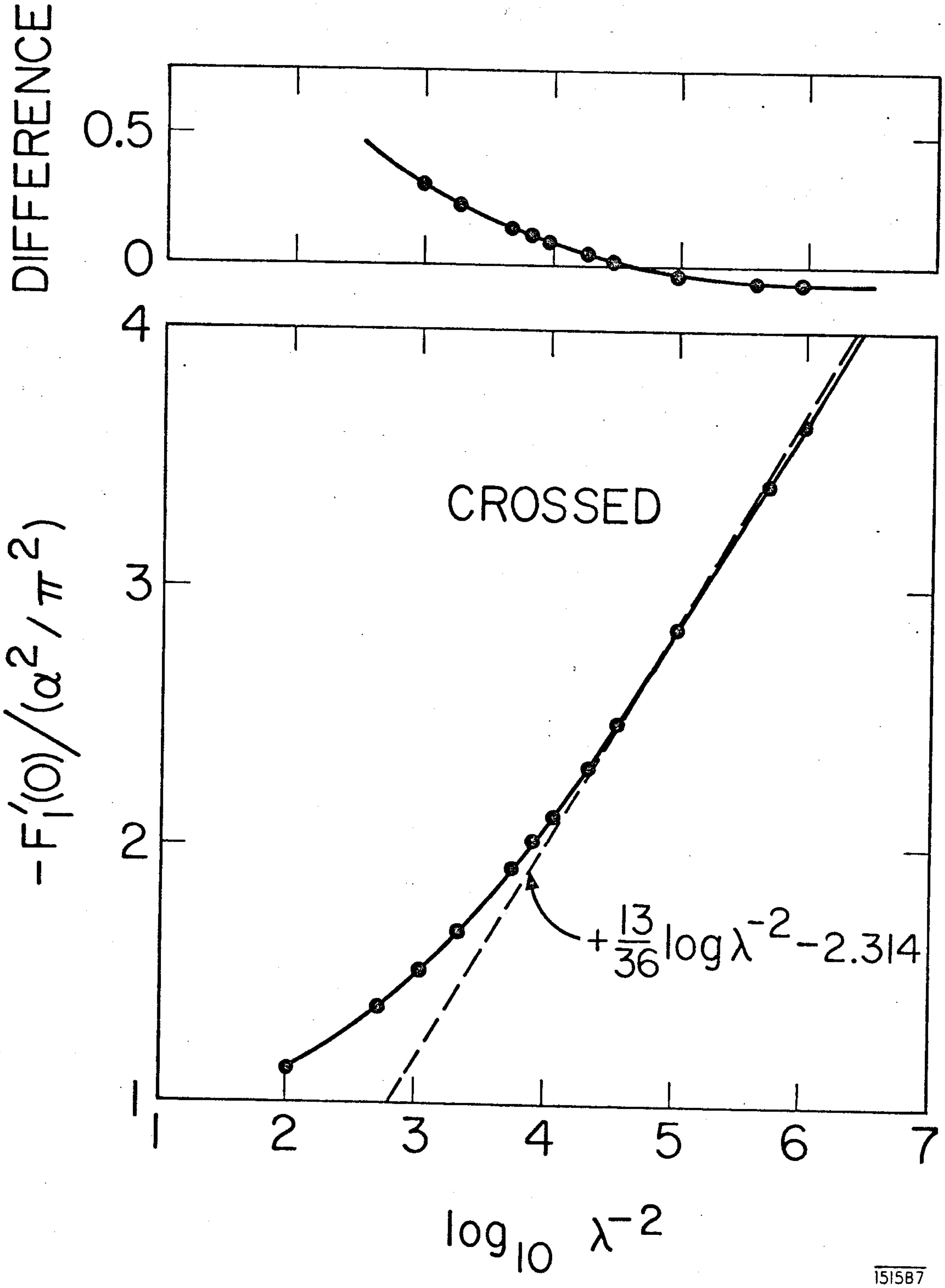

DIFFERENCE
0.5
0
4
3
2
1
CROSSED
$-F_1'(0)/(\alpha^2/\pi^2)$
$+\frac{13}{36}\log\lambda^{-2}-2.314$
1
2
3
4
5
6
7
$\log_{10}\lambda^{-2}$
1515B7

Fig. 8

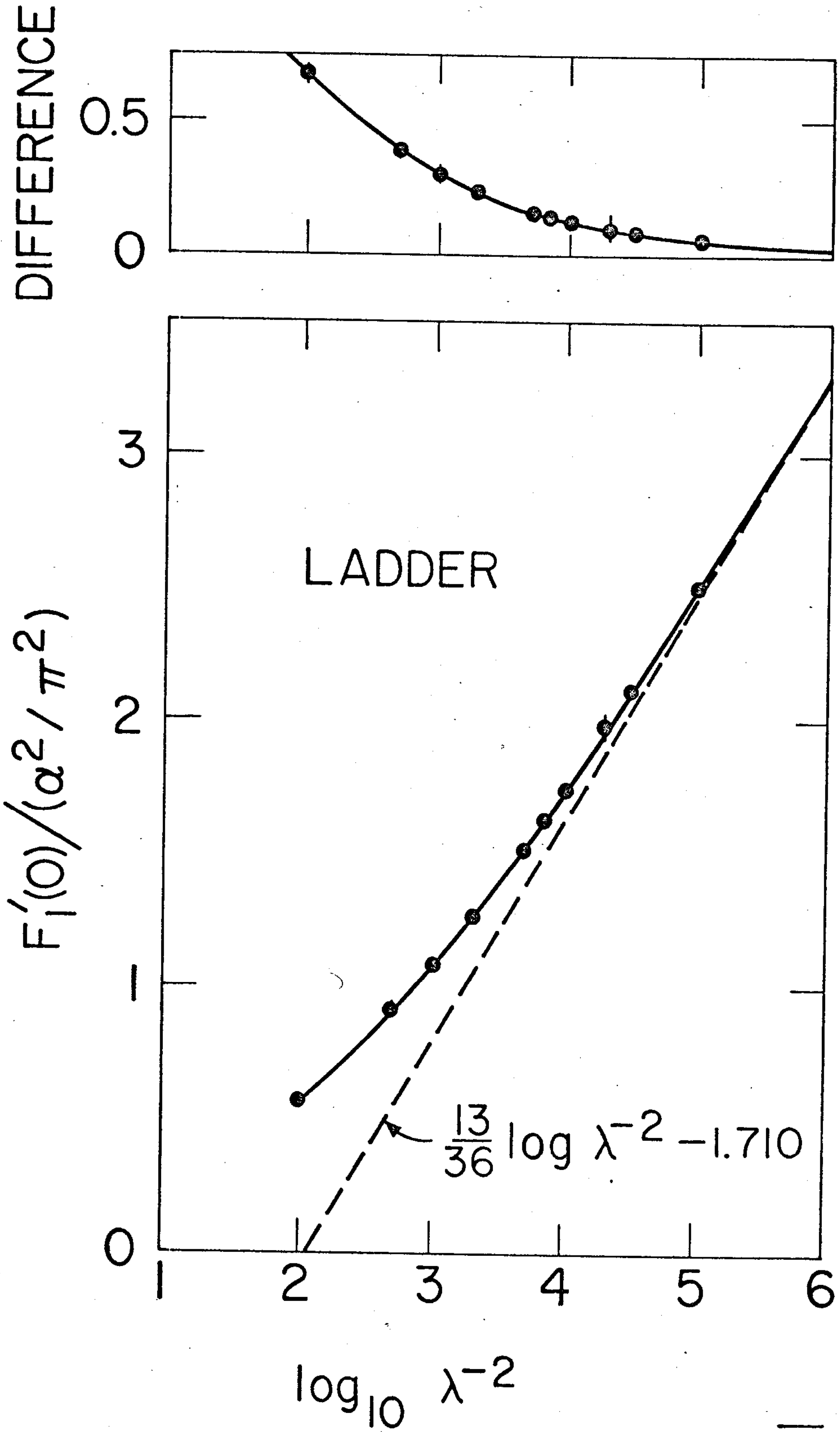
DIFFERENCE
0.5
0
LADDER
$F_1'(0)/(\alpha^2/\pi^2)$
3
2
1
0
$\frac{13}{36} \log \lambda^{-2} - 1.710$
1
2
3
4
5
6
$\log_{10} \lambda^{-2}$

151581

Fig. 9

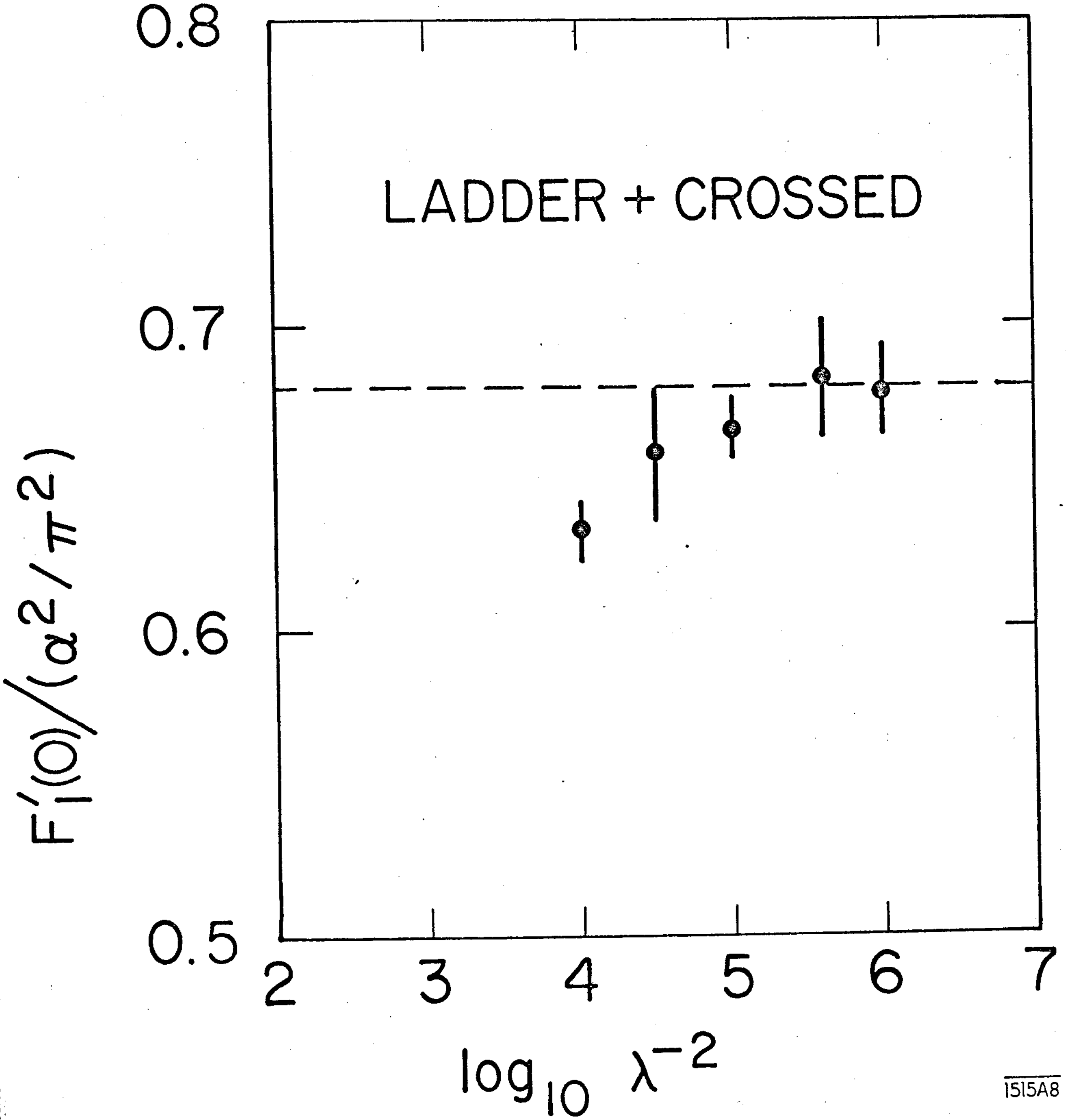

LADDER + CROSSED
0.8
0.7
0.6
0.5
2
3
4
5
6
7
$F_1'(0)/(\alpha^2/\pi^2)$
$\log_{10} \lambda^{-2}$
1515A8

Fig. 10